Formation of PS-*b*-P4VP/Formic Acid Core−Shell Micelles in Chloroform with Different Core Densities

Ximei Yao, Daoyong Chen,* and Ming Jiang

Department of Macromolecular Science and The Key Laboratory of Molecular Engineering of Polymers, Fudan University, Shanghai 200433, China

Received: December 24, 2003; In Final Form: February 25, 2004

Micellization of the complexes of polystyrene-*b*-poly(4-vinylpyridine) (PS-*b*-P4VP) with formic acid (FA) takes place in chloroform, leading to regular aggregates. The resultant aggregates were characterized by dynamic light scattering (DLS), static light scattering (SLS), scanning electron microscopy (SEM), and ^{1}H NMR. The variation of the average radius of gyration ($\langle R_g \rangle$) of the aggregates with the molar ratio of FA to the pyridine units of the copolymer (MR) was used as an important clue for the characterization of the morphologies. It is shown that the aggregates have a morphology of conventional micelles or micelles with a low-density core rather than vesicles, depending on the value of MR. Although the conventional micelles are most commonly obtained aggregates via micellization of a block copolymer in its selective solvent, the micelles with a low-density core (similar to a swollen physical microgel) are novel core−shell nanoparticles, which have been rarely reported and are expected to have a great potential for applications.

Introduction

Micellization of block copolymers in solutions and the resultant polymeric micelles have attracted considerable interest in both theoretical and applied research fields.[1] While the micellization of block copolymers in selective solvents has been deeply and widely studied, great efforts have been made to search for new routes to the micellization. It was found that self-assembly of block copolymers can also be realized by altering the temperature,[2] changing the pH values,[3] and chemically modifying one of the blocks of a copolymer.[4] In addition, inter-polymer complexation due to electrostatic interaction[5] or hydrogen bonding[6] can also lead to the micellization.

Recently, the behaviors of the complexes of block copolymers with low-molecular-mass compounds (LMC**)** (including surfactants and other molecules with a polar head and a nonpolar tail) were studied. The micellization of the complexes of block copolymers/LMC has shown great controllability since the amount of LMC is easy to control, the binding between block copolymers and LMC is sensitive to the changes in the environment, and there are wide varieties of LMC to choose from.[7] This makes the systems of block copolymers/LMC very promising in addressing various theoretical and practical problems. It was reported that in aqueous medium, the interaction between LMC and a block copolymer might result in micellar clusters (including precipitation)[8a] or vesicles,[8b,8c] depending on the dispersion state of the block copolymer before the mixing with LMC. The aggregation of the insoluble surfactant tails is responsible for the micellization or the precipitation. While in low polar organic solvents, since the nonpolar tails of LMC are soluble in the medium, the behaviors of the complexes are quite different. Due to the fact that the block copolymers capable of forming complexes with LMC contain at least a block with polar groups, the binding with LMC usually improves their solubility in low-polarity organic solvents.[9] Therefore, regular aggregates resulting from the complexation between block copolymers and LMC in organic solvents have been seldom reported. To take full advantages of these systems, it is obviously significant to realize the micellization of the complexes in organic solvents. Our previous work[10] presented a preliminary result on the behaviors of complexes of polystyrene-*b*-poly(4-vinylpyridine) (PS-*b*-P4VP) with linear aliphatic acids in chloroform. It is shown that when the lipophilic tails of the acids are removed, the complex self-assembles forming vesicles. This is one of a few examples, to our knowledge, to obtain regular nano-aggregates in a low-polarity medium through the complexation-induced micellization of a block copolymer/LMC complex.

Here we present our entirely new results on the micellization of PS-*b*-P4VP/formic acid (FA) complexes in chloroform and the characterization of the resultant aggregates. When the copolymer with the length ratio (LR) of the PS block to the P4VP block of 2/1 is used, at the concentration of the copolymer of 1.0 mg/mL, conventional micelles or the micelles with a low-density core (such as a swollen physical microgel) are obtained, depending on the molar ratio (MR) of FA to the pyridine units. We will also lay emphasis on the characterization of the micelles with a low-density core, which may be a little bit confusing since no unique characteristics have been established for the characterization of these micelles.

Experimental Section

Materials. PS-*b*-P4VP was synthesized and characterized according to procedures described in ref 11. The weight average molecular weights of the PS block, P4VP block, and the molecular weight polydispersity index of the PS precursor are 51 000, 25 800, and 1.09, respectively. FA was distilled after refluxing in phthalic anhydride for more than 12 h before use. Chloroform of analytical grade was used as received. The homopolymer P4VP was synthesized via a radical polymerization.

Micellization of PS-*b*-P4VP/FA. The block copolymer was dissolved in $CHCl_3$ for at least 2 days before use. Then, FA/$CHCl_3$ solution was added dropwise into each of the copolymer

10.1021/jp038000j CCC: $27.50 © 2004 American Chemical Society
Published on Web 04/02/2004

solutions under ultrasonic until the designed MR was reached. The concentrations of the block copolymer in the final solutions are 1.0 mg/mL, and MR in the final solutions are 1/6, 1/5, 1/3, 1/2, 2/3, and 1/1, respectively.

Laser Light Scattering (LLS). A modified commercial light scattering spectrometer (ALV/SP-125) equipped with an ALV-5000 multi-τ digital time correlator and an ADLAS DPY425 II solid-state laser (output power = 400 mW at $\lambda = 532$ nm) was used. In dynamic LLS (DLS), the line-width distribution $G(\Gamma)$ can be calculated from the Laplace inversion of intensity−intensity−time correlation function $G^{(2)}(q,t)$. The inversion was carried out by the CONTIN program. $G(\Gamma)$ can be converted into a transitional diffusion coefficient distribution $G(D)$ or a hydrodynamic radius distribution $f(R_h)$ via the Stokes−Einstein equation, $R_h = (k_B T/6\pi\eta)D^{-1}$, where k_B, T, and η are the Boltzmann constant, the absolute temperature, and the solvent viscosity, respectively. All the DLS measurements were performed at 25 ± 0.1 °C and at a scattering angle 90° as no remarkable scattering angle dependence of the $\langle R_h \rangle$ of the micelles was observed. All the micelle solutions were measured directly *without dilution*, and the solutions were clarified using a 0.45 μm Millipore filter before the measurements. In Static Light Scattering (SLS), the angular dependence of the excess absolute time-averaged scattered intensity of a very dilute dispersion, i.e., the Rayleigh ratio Rvv(q), can lead to the weight-averaged molar mass Mw, the second virial coefficient A2, and the z-averaged root-mean square radius of gyration $\langle R_g^2 \rangle_z^{1/2}$, where q is the scattering vector.

Scanning Electron Microscopy (SEM). SEM observations were conducted on a Philips XL30 at an accelerating voltage of 25 kV. The specimens for SEM observations were prepared by depositing a drop of the solutions (ca. 5 μL) onto a glass slide.

^{1}H NMR Measurements. The ^{1}H NMR measurements were performed on a Bruker DMX500 spectrometer in $CDCl_3$ using TMS as an internal reference.

Results and Discussion

In our previous study,[10] we have demonstrated that the complexes of PS-*b*-P4VP/linear aliphatic acids form in chloroform due to the hydrogen bonding between the pyridine units and the carboxyl groups. The stoichiometric complexes of PS-*b*-P4VP with stearic acid, decanoic acid, and acetic acid, respectively, can be molecularly dispersed in the solution; while the complex of PS-*b*-P4VP with formic acid will self-assemble in chloroform, forming regular nano-aggregates. The lack of the hydrocarbon tails and the higher acidity of FA (as compared with other aliphatic acids) make the complexed units of pyridine/FA insoluble in the low-polarity medium, being responsible for the micellization. It was found that when the block copolymer with the length ratio (LR**)** of the PS block to the P4VP block being 1.15/1 was used, only vesicles were produced from the micellization.

In the present study, the average molecular weights (Mw) of the PS and P4VP blocks of the block copolymer used are 51 000 and 25 800, respectively, so the LR is ca. 2/1. Although the micellization takes place as well upon mixing the copolymer with FA at the concentration of the PS-*b*-P4VP of 1.0 mg/mL, the results are quite different from what we obtained previously. We first characterized the resultant aggregates by DLS and SLS. The average hydrodynamic radius ($\langle R_h \rangle$), the average radius of gyration ($\langle R_g \rangle$), and the values of $\langle R_g \rangle / \langle R_h \rangle$ of the resultant aggregates at different MR are presented in Figure 1.

From the data in Figure 1, it seems that the association takes place when MR is 1/6, since the $\langle R_h \rangle$ is much larger than that of an individual copolymer chain ($\langle R_h \rangle$ of the pure copolymer in chloroform was measured to be ca. 10 nm). Although no remarkable change in $\langle R_h \rangle$ with MR is found in the range of MR between 1/6 and 1/2, it increases rapidly in the range between 1/2 and 2/3. Then, $\langle R_h \rangle$ increases slowly with MR. The change in $\langle R_g \rangle$ with MR is quite different. $\langle R_g \rangle$ drops from 51 to 32 nm, while MR increases from 1/6 to 1/5; subsequently, it remains nearly unchanged with the further increase of MR. As a result, $\langle R_g \rangle / \langle R_h \rangle$ drops from 1.8 to 1.1 when MR increases from 1/6 to1/5, then it stays in the range from 1.1 to 1.2 until MR is 1/2 and drops again to 0.58 when MR increases to 2/3.

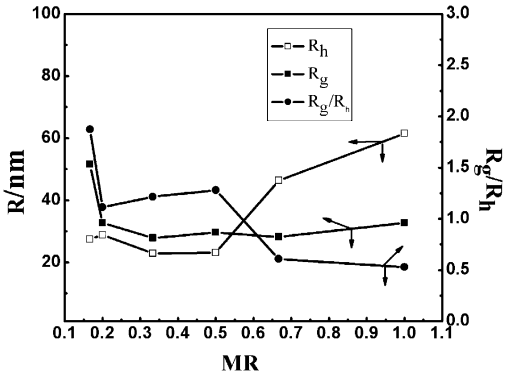

Figure 1. The values of $\langle R_h \rangle$, $\langle R_g \rangle$, and $\langle R_g \rangle / \langle R_h \rangle$ of the aggregates obtained at different MR. The concentration of the block copolymer is 1.0 mg/mL.

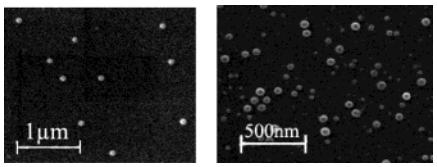

Figure 2. SEM images of nano-aggregates obtained at the concentration of PS-*b*-P4VP of 1.0 mg/mL and MR of 1/1 (Figure 2a) and 1/3 (Figure 2b).

First, the values of $\langle R_g \rangle / \langle R_h \rangle$ can give us information about the morphology of the resultant aggregates. Theoretically, for a uniform nondraining solid sphere, a nondraining thin shell vesicle and a random coil, the ratios of $\langle R_g \rangle / \langle R_h \rangle$ are 0.774, 1.0, and 1.5∼1.8, respectively.[12,13] While experimentally, for a polymeric micelle, $\langle R_g \rangle / \langle R_h \rangle$ is often less than 0.774 since the density of the core is remarkably higher than that of the shell;[2a,14] for a polymeric vesicle or a hollow sphere, $\langle R_g \rangle / \langle R_h \rangle$ may be less or larger than 1.0, depending on the thickness and the density of the wall.[12] In this work, $\langle R_g \rangle / \langle R_h \rangle$ at MR of 1/6 is 1.8, being at the upper end of the range for a random coil; in the range of MR between 1/5 and 1/2, $\langle R_g \rangle / \langle R_h \rangle$ is around 1.1, being among the range for *a vesicle* or *a hollow sphere*; when MR is larger than or equal to 2/3, $\langle R_g \rangle / \langle R_h \rangle$ is much less than 0.774, showing a feature as *a conventional micelle*. Accordingly, we make preliminary assumptions that the aggregates formed at MR values of 1/6, 1/5−1/2, 2/3−1/1 are loosely entangled polymer chains, vesicles, or micelles with a low-density core, conventional micelles, respectively.

Our SEM observations have proved that the nano-aggregates formed at MR between 2/3 and 1/1 are conventional micelles, as the aggregates in the SEM images show a morphology of typical conventional micelles (Figure 2a). However, the SEM images of aggregates obtained at MR between 1/5 and 1/2 are different from that of typical vesicles (Figure 2b).[1a,1b,1c,1d,10] From Figure 2b one can see that, although the morphology of the aggregates is not so similar to that of vesicles, there is a remarkable contrast between the central and the edge parts of

an aggregate in the SEM image, exhibiting a concave central area. This makes the morphology of the aggregates obtained at MR between 1/5 and 1/2 different from that of conventional micelles as well. Therefore, we assume these aggregates as the micelles with a core of a low density (a core similar to a swollen physical microgel). It is speculated that the core will shrink and collapse more upon drying, when compared with a solid core. This will lead to the concave in the central area and the contrast between the central area and the edge part in the SEM image, resulting in a morphology intermediate between those of a vesicle and a conventional micelle. Therefore, we are inclined to consider the aggregates obtained at MR between 1/5 and 1/2 as the micelles with a core of a low chain density rather than vesicles. This consideration is consistent with the assumption made according to the values of $\langle R_g \rangle / \langle R_h \rangle$.

Furthermore, as is mentioned above, the $\langle R_g \rangle$ remains nearly constant after MR is larger than or equal to 1/5 (Figure 1). This phenomenon can only be explained by assuming the aggregates formed in the range of MR between 1/5 and 1/2 as micelles with a low-density core rather than as vesicles. It is stated that $\langle R_h \rangle$ is sensitive to the hydrodynamic draining, while $\langle R_g \rangle$ depends only on the spatial chain distribution.[2a,15] Since the spatial chain distributions of vesicles and micelles are very different,[16] it is unimaginable that the morphology of aggregates changes from vesicles to conventional micelles while the $\langle R_g \rangle$ of these aggregates changes little. It has been proved[10] that the aggregates obtained via the micellization of PS-*b*-P4VP/FA in chloroform are with the PS block as the shell and complexed P4VP block as the core. When MR is in the range between 1/5 and 1/2, more than one-half of pyridine units are free from the connection with FA molecules and these units should be soluble. So, the core may be to a certain extent like "a soluble network" and the chain density is low, making the aggregates similar in $\langle R_g \rangle / \langle R_h \rangle$ values to hollow spheres or vesicles and their morphology in SEM images intermediate between those of vesicles (or hollow spheres) and conventional micelles. While MR increases further from 1/2 to 2/3, a majority of the pyridine units are complexed with FA and the P4VP block chains may become entirely insoluble. So, the micelles formed at MR larger than or equal to 2/3 are conventional micelles. This agrees well with the results obtained from the experiment of mixing the homopolymer poly(4-vinylpyridine) (P4VP) with FA in chloroform. P4VP/FA at MR less than or equal to 1/2 is soluble nanogels, while P4VP/FA at MR larger than or equal to 2/3 forms a precipitate in chloroform. It is possible that, similar to the case reported by Kabanov and Eisenberg,[9] due to the binding with small molecules, the rigidity of P4VP chains increases and their conformation does not change considerably with the variation of MR (MR is larger than or equal to 1/5). Therefore, we suppose that each of the copolymer chains in the aggregates is approximately radially oriented (as is described in ref 2a), and the conformation of the chains does not change remarkably with MR, the spatial mass distribution (which is also the radial mass distribution when we suppose that the copolymer chains are radially oriented in a spherical aggregate), as well as $\langle R_g \rangle$ should not vary considerably with MR. It is understandable that when the core changes from a low-density one to a solid one, the drainability will decreases and the $\langle R_h \rangle$ increases remarkably.[23]

Our further ^{1}H NMR measurements also support our assumptions on the structures of the aggregates obtained at different MR. The spectra of the complexes at MR of 0, 1/3, and 1/1 are shown in Figure 3. For clarity, only the spectra between 5.5 and 9.0 ppm are shown.

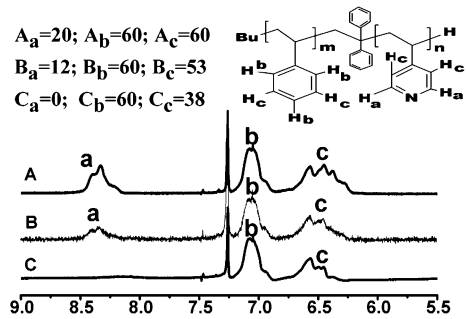

Figure 3. ^{1}H NMR spectra of FA/PS-*b*-P4VP in $CDCl_3$ at different MR of 0 (A), 1/3 (B) and 1/1 (D). In the inset, K_i refers to the peak area of peak i in spectrum K.

As is mentioned before, in chloroform, the complexed units of pyridine/FA are insoluble and associate to form the core of the aggregates, driving the micellization. These aggregated pyridine units will lose their mobility as well as their signals in the spectra.[17] However, all the PS block chains, as the shell of the aggregates, should remain in a soluble state and their signals' intensities do not change with MR. From the spectra one can see that, with the addition of MR, the relative intensity of peak **b** assigned to the hydrogen atoms H_b (inset) in the benzene rings only does not change while those of peak **a** and peak **c**, which are associated to H_a in the pyridine rings and H_c in both the pyridine and benzene rings, respectively, decrease. It is noted that when MR is 1/3, the pyridine signals are still visible with considerable strengths, indicating the presence of many movable pyridine units (peak **a** and peak **c** in spectrum B). Therefore, it is reasonable to think that a large part of the pyridine units remains in a soluble state in the core of the aggregates. This implies that the core of these aggregates is in a state like a swollen microgel; the density must be low. While MR is 1/1, nearly all the pyridine units are seriously restricted and lose their signals, so peak **a** disappears and the intensity ratio of **b** to **c** becomes close to 3/2, which is the number ratio of the H_b to H_c in the benzene rings (spectrum C). Obviously, the aggregates at MR of 1/1 are in fact the conventional micelles.

In our previous work, it was noted that a high field shift occurred in peak **a** with the addition of FA.[10] This is attributed to the fact that the detectable pyridine rings are closely surrounded by aggregated ones, which partially shield the outer magnetic field for those detectable pyridine rings. However, peak **a** in spectrum B of Figure 3 in this study does not show any high or low field shifts. This reflects the low-density nature of the core of the micelles, in which the aggregated pyridine rings should not so closely surround the detectable ones.

According to SEM observations, the size distributions of the conventional micelles are narrow, whereas those of the micelles with a low-density core are broad, much broader than those of the conventional micelles, as indicated in Figure 2. It is reported that the complexation of the pyridine units with FA in chloroform is irreversible; the complexation occurs simultaneously upon the mixing of the copolymer with FA.[10] When MR is relatively small, due to the limitation of the diffusion of FA in the system, the different individual copolymer chains may have different molar ratios (denoted as MR_{ind}) of the pyridine units to FA. In this system, there may be a small part of the complexed copolymer chains with the MR_{ind} values much different from the MR (for example, some of them possibly have MR_{ind} values less than 1/6). It is possible that the behavior of these copolymer chains is different from the others, and the micellization of these chains may lead to micelles with the sizes different from those of the majority of micelles. This is

speculated to be responsible for the broad size distributions of the micelles with a low-density core. In addition, the polydispersity indexes (PDIs) of the aggregates at MR of 1/1, 2/3, 1/2, 1/3, 1/5, and 1/6 are measured by DLS to be 0.06, 0.08, 0.10, 0.10, 0.10, and 0.14, respectively.[18] It is reported that for monodisperse or nearly monodisperse samples, the PDI is close to 0 (0.00 to 0.02); for narrow size distributions, it ranges from 0.02 to 0.10, and for broader size distributions, it exceeds 0.10.[19] On the basis of DLS measurements, the size distributions of the conventional micelles are narrow, findings which are consistent with those observed by SEM. However, for the micelles with a low-density core, the size distributions measured by DLS are intermediate between the narrow and the broad, narrower than those observed by SEM (as indicated by Figure 2b). It is worth noting that the light scattering intensity is proportional to both the number (n) of scatterers and the square of the scatterer's mass, and the scatterer's mass is proportional to the cube of its radius; the calculation of the PDIs is based on the intensity-weighted distribution of the hydrodynamic radius.[20] We have noted that the broad size distributions in the SEM images result from the existence of some small particles with a radius ca. 10 nm (as indicated in Figure 2b). However, on the basis of the discussion above, these small aggregates should not affect the PDIs considerably.[20] As a result, for the micelles with a low-density core, the size distributions measured by DLS are narrower than those observed by SEM.

As is mentioned before, when the copolymer with the LR of the PS block to the P4VP block being 1.15/1 is used,[10] the micellization of PS-*b*-P4VP/FA leads to vesicles; while in this study, the LR is 2/1, it results in micelles. The increase in the LR leads to the change in the morphology of resultant nano-aggregates from vesicles to micelles. This phenomenon can be well understood by considering a balance between three major forces acting on the system: the stretching of the core-forming blocks, the interfacial tension between the core and the solvent, and the intercorona repulsion.[21] For example, the decrease in the length of the shell-forming block will weaken the intercorona repulsion. According to Eisenberg, when the intercorona repulsion becomes weaker, the core size can increase in order to decrease the interfacial energy between the core and the solvent. However, the increase of the core size is restricted by an entropic penalty resulting from the stretching of the core-forming block. At some point, as the strength of the repulsive interactions among corona chains decreases and the stretching of the PS chains increases, the aggregates change their morphology from micelles to vesicles in order to reduce the entropic penalty.[21,22]

In the present study, the micellization of PS-*b*-P4VP/FA, at MR greater than or equal to 1/5, leads to the micelles with complexed P4VP as the core and PS as the shell. The aggregation of the insoluble pyridine/FA units is the driving force. It is reasonable to assume the core as a particle of "physically cross-linked P4VP". The increase in MR should result in the increase in the "cross-linking density". When MR is relatively small, the "cross-linking density" should be low, and the "physically cross-linked P4VP" in the solvent should be swollen due to the existence of a relatively large amount of soluble pyridine units, which are free from binding FA, within it. While when the MR is close to 1/1, most of the pyridine units are bound with FA and become insoluble, therefore, the "physically cross-linked P4VP" becomes solid. As a result, with the increase of MR, the morphology of the aggregates changes from the micelles with a low-density core to the conventional micelles. We would like to mention here that the micellization of block copolymers usually leads to spherical aggregates, although the aggregates with other morphologies have been reported. As to the spherical aggregates, only conventional micelles and vesicles have been reported. In some cases, such as present study, there are obviously two components, one of which is soluble while the other is insoluble, in the core of the aggregates. If the soluble component exists in large amount and is randomly distributed within the insoluble one, the core of the aggregates perhaps adopts a structure similar to a swollen microgel and should have a low density. With such a hybrid-like core, the aggregates should have properties different from either the conventional micelles or vesicles.

Conclusion

The micellization of PS-*b*-P4VP/FA (the LR of the copolymer is 2/1) at concentration of the copolymer of 1.0 mg/mL leads to regular aggregates when MR is larger than or equal to 1/5. When MR is less than or equal to 1/2, the core of the micelles is in fact like a microgel. The conventional micelles are commonly reported nano-aggregates for the systems of block copolymers in the selective solvents. However, the micelles with a core similar to a swollen physical gel have not been reported yet. In some cases, they may be confused with vesicles or conventional micelles. In principle, the low-density core may provide more space for encapsulation, and the existence of the multi-core-forming components may be helpful to anchor or enrich some desired species in the core. All these features will make the micellization of a block copolymer/LMC promising for future applications. Besides, this work may initiate the interest to further confirm the existence of such micelles in other systems and be helpful to establish a fundamental basis for the characterization of such aggregates.

Acknowledgment. The authors are grateful to Professor Chi Wu and Professor Guangzhao Zhang of University of Science and Technology in China for their kind help in completion of this work. This work has been supported by National Science Foundation of China 50273006.

References and Notes

(1) (a) Zhang, L. F.; Eisenberg, A. *Science* **1995**, *268*, 1728. (b) Zhang, L. F.; Eisenberg, A. *Science* **1996**, *272*, 1777. (c) Jenekhe, S. A.; Chen, X. L. *Science* **1998**, *279*, 1903. (d) Discher, B. M.; Won, Y. Y.; Ege, D. S.; Lee, J. C. M.; Bates, F. S.; Discher, D. E.; Hammer, D. A. *Science* **1999**, *284*, 1143. (e) Kabanov, A. V.; Kabanov, V. A. *Adv. Drug Delivery Rev.* **1998**, *30*, 49. (f) Zhang, G. Z.; Liu, L.; Zhao, Y.; Ning, F. L.; Jiang, M.; Wu, C. *Macromolecules* **2000**, *33*, 6340.

(2) (a) Tu, Y.; Wan, X.; Zhang, D.; Zhou, Q.; Wu, C. *J. Am. Chem. Soc.* **2000**, *122*, 10201; (b) Svensson, M.; Alexandridis, P.; Linse, P. *Macromolecules* **1999**, *32*, 637; (c) Bütün, V.; Armes, S. P.; Billingham, N. C. *Macromolecules* **2001**, *34*, 1148.

(3) (a) Liu, S. Y.; Billingham, N. C.; Armes, S. P. *Angew. Chem., Int. Ed.* **2001**, 40, 2328; (b) Gohy, J.; Antoun, S.; Jerome, R. *Macromolecules* **2001**, *34*, 7435.

(4) Wu, C.; Niu, A. Z.; Leung, L. M.; Lam, T. S. *J. Am Chem. Soc.* **1999**, 121, 1954.

(5) (a) Harada, A.; Kataoka, K. *Macromolecules* **1995**, *28*, 5294; (b) Kabanov, A. V.; Bronich, T. K.; Kabanov, V. A.; Yu, K.; Eisenberg, A. *Macromolecules* **1996**, *29*, 6797.

(6) (a) Wang, M.; Zhang, G. Z.; Chen, D. Y.; Jiang, M.; Liu, S. Y. *Macromolecules* **2001**, *34*, 7172; (b) Wang, M.; Jiang, M.; Ning, F. L.; Chen, D. Y.; Liu, S. Y.; Duan, H. W. *Macromolecules* **2002**, *35*, 5980.

(7) (a) Ruokolainen, J.; Mäkinen, R.; Torkkeli, M.; Mäkelä, T.; Serimaa, R.; ten Brinke, G.; Ikkala, O. *Science* **1998**, *280*, 557; (b) Ruokolainen, J.; ten Brinke, G.; Ikkala, O. *Adv. Mater.* **1999**, *11*, 777; (c) Ruokolainen, J.; Torkkeli, M.; Serimaa, R.; Komanschek, E.; ten Brinke, G.; Ikkala, O. *Macromolecules* **1997**, *30*, 2002; (d) de Moel, K.; Alberda van Ekenstein, G. O. R.; Nijland, H.; Polushkin, E.; ten Brinke, G.; Mäki-Ontto, R.; Ikkala, O. *Chem. Mater.* **2001**, *13*, 4580.

(8) (a) Lysenko, E. A.; Bronich, T. K.; Slonkina, E. V.; Eisenberg, A.; Kabanov, V. A.; Kabanov, A. V. *Macromolecules* **2002**, *35*, 6351. (b) Kabanov, A. V.; Bronich, T. K.; Kabanov, V. A.; Yu, K.; Eisenberg, A. *J.*

Am. Chem. Soc. **1998**, *120*, 9941; (c) Bronich, T. K.; Ouyang, M.; Kabanov, V. A.; Eisenberg, A.; Szoka, F. C., Jr.; Kabanov, A. V. *J. Am. Chem. Soc.* **2002**, *124*, 11872.

(9) (a) Bakeev, K. N.; Lysenko, E. A.; MacKnight, W. J.; Zezin, A. B.; Kabanov, V. A. *Colloids Surf., A: Physicochemical and Engineering Aspects* **1999**, *147*, 263; (b) Lysenko, E. A.; Bronich, T. K.; Slonkina, E. V.; Eisenberg, A.; Kabanov, V. A.; Kabanov, A. V. *Macromolecules* **2002**, *35*, 6344.

(10) Peng, H.; Chen, D.; Jiang, M. *Langmuir* **2003**, *19*, 10989.

(11) Thurmond, K. B., II; Kowalewski, T.; Wooley, K L. *J. Am. Chem. Soc.* **1997**, *119*, 6656.

(12) Duan, H. W.; Chen, D. Y.; Jiang, M.; Gan, W. J.; Li, S. J.; Wang, M.; Gong, J. *J. Am. Chem. Soc.* **2001**, *123*, 12097.

(13) Zhang, G. Z.; Liu, L.; Zhao, Y.; Ning, F. L.; Jiang, M.; Wu, C. *Macromolecules* **2000**, *33*, 6340.

(14) Moffitt, M.; Yu, Y.; Nguyen, D.; Graziano, V.; Schneider, D. K.; Eisenberg, A. *Macromolecules* **1998**, *31*, 2190.

(15) Zhang, G. Z.; Wu. C. *Phys. Rev. Lett.* **2001**, *86*, 822.

(16) Stewart, S.; Liu, G. *Chem. Mater.* **1999**, *11*, 1048.

(17) Chen, D. Y.; Peng, H. S.; Jiang, M. *Macromolecules* **2003**, *36*, 2576.

(18) Chu, B.; Wang, Z.; Yu, J. *Macromolecules* **1991**, *24*, 6832.

(19) Bronich, T. K.; Popov, A. M.; Eisenberg, A.; Kabanov, V. A.; Kabanov, A. V. *Langmuir* **2000**, *16*, 481.

(20) Li, X. Y.; He, X.; Ng, A. C. H.; Wu, C. Ng, D. K. P. *Macromolecules* **2000**, *33*, 2119.

(21) Zhang, L. F.; Eisenberg, A. *Macromolecules* **1996**, *29*, 8805.

(22) Shen, H.; Eisenberg, A. *Macromolecules* **2000**, *33*, 2561.

(23) The apparent values of $\langle Mw \rangle$ of the aggregates should be important to indicate the change in the density of the core. In fact, the $\langle Mw \rangle$ of the aggregates obtained at MR = 1/1 is much larger than those at MR $\leq$ 1/2, according to the SLS measurements. However, it should be mentioned that the values might not be precise enough, since the extrapolation of $c \rightarrow 0$ was not made in fear that the further dilution might change the structure and morphology of the aggregates. For this reason, the change in $\langle Mw \rangle$ of the aggregates with MR is not regular and the values are not shown here. It is widely accepted that the $\langle R_g \rangle$ values are precise without the extrapolation.